

# Characterization of a conical intersection between the ground and first excited state for a retinal analog<sup>☆</sup>

F. Molnar<sup>a</sup>, M. Ben-Nun<sup>b</sup>, T.J. Martínez<sup>a,b,\*</sup>, K. Schulten<sup>a,c,1</sup>

<sup>a</sup>Beckman Institute, University of Illinois at Urbana-Champaign, Urbana, IL 61801, USA

<sup>b</sup>Department of Chemistry, University of Illinois at Urbana-Champaign, Urbana, IL 61801, USA

<sup>c</sup>Department of Physics, University of Illinois at Urbana-Champaign, Urbana, IL 61801, USA

## Abstract

Ab initio complete active space SCF calculations have been carried out to investigate the first excited electronic state of a retinal protonated Schiff base analog: all-*trans*-3,7-dimethylnona-2,4,6,8-tetraenmethyliminium cation. This model of the retinal chromophore in bacteriorhodopsin includes five conjugated double bonds as well as both pertinent backbone methyl groups. The excited state minimum that is relevant for isomerization in bacteriorhodopsin is investigated and is found to be in very close proximity to a Jahn–Teller conical intersection. The two (global) coordinates that are most effective in promoting efficient internal conversion back to the ground electronic state (by lifting the degeneracy between the ground and first excited state) are identified and discussed, and the distribution of the positive charge in the retinal analog as a function of these two coordinates is investigated. © 2000 Elsevier Science B.V. All rights reserved.

**Keywords:** Bacteriorhodopsin; Retinal protonated Schiff base; Polyenes; Photoisomerization; Quantum chemistry; Conical intersection

## 1. Introduction

The all-*trans* retinal protonated Schiff base (RPSB) is the chromophore of bacteriorhodopsin (bR), a trans-membrane protein that acts as a light-driven proton pump in *Halobacterium salinarium*, converting light energy into a proton gradient. The bR protein contains seven  $\alpha$ -helices and its prosthetic group is attached to the protein via a Schiff base linkage to a lysine side chain (Lys216). Upon absorption of light the chromophore undergoes a photoisomerization process and the thermal reversal of this reaction is coupled to the translocation of a proton from the cytoplasmic side

to the extracellular side of the protein. As its name indicates, bR is closely related to the rhodopsin family of proteins, which act as primary light detectors in the vision process of higher life forms.

Due to its relatively simple structure (as compared to other bioenergetic proteins involved in proton pumping), its stability, and its strong spectral shifts in the 400–600 nm range (which permit identification of reaction intermediates), bR has been an ideal system for investigations of vectorial proton translocation through membranes. For reviews and summary of the theoretical work see Refs. [1–5]. Despite this barrage of investigations the riddle of bR's proton pump mechanism, how a photoreaction and its thermal reversal is coupled to vectorial proton translocation has not been answered.

One of the reasons for the elusiveness of the mechanism of bR's proton pump is our lack of

<sup>☆</sup> Presented at the 5th World Congress of Theoretically Oriented Chemists (WATOC), Imperial College, London, 1–6 August, 1999.

\* Corresponding author.

<sup>1</sup> Corresponding co-author.

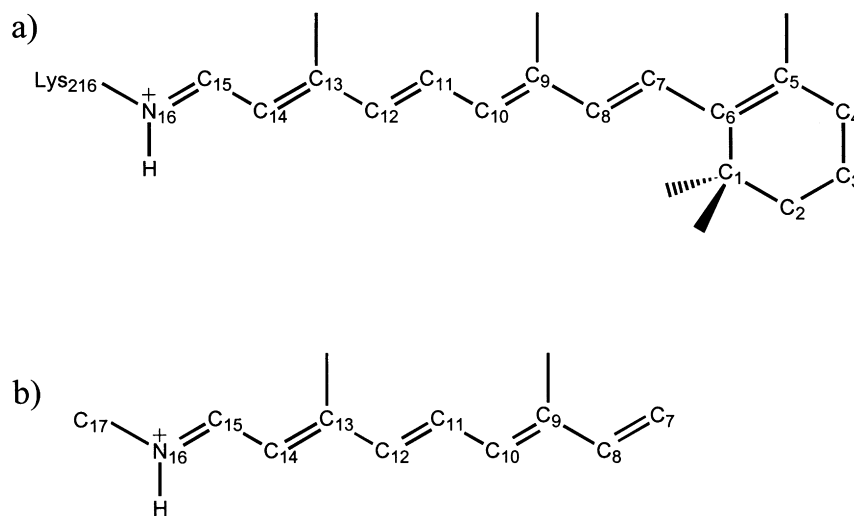


Fig. 1. Structure and atom labeling of retinal protonated Schiff base (panel a) and its analog: all-*trans*-3,7-dimethylnona-2,4,6,8-tetraenyliminium cation (panel b).

complete knowledge of the exact nature of the photoproduct that triggers proton release from retinal to Asp85, which is connected to the extracellular side through a water channel. In order to determine the photoproduct in molecular dynamics simulations, starting from the well-known ground state structure of bR [6,7], accurate ground and excited state potential energy surfaces are required. In order to provide such surfaces, we consider in this paper an *isolated* retinal analog model that permits us to characterize the first excited state in vicinity of the minimum and conical intersection (CI) (between the ground and first excited state) associated with isomerization around the C<sub>13</sub>=C<sub>14</sub> bond (see Fig. 1). The characterization of the first excited state will enable us to extend and improve earlier quantum mechanical studies of the photoreaction dynamics in the protein reported in [8]. Such studies of the first step in the photocycle are part of our investigations of the early intermediates in the photocycle and the role of water molecules within the protein interior [9–15].

A faithful description of bR's photodynamics and of the resulting photoproducts depends on the availability of accurate potential-energy surfaces (PESs) and on the ability to treat the quantum mechanical nature of the nuclear motion. The initial photoinduced isomerization of retinal from its all-*trans* to 13-*cis* structure is widely believed to occur on a sub-picose-

cond time scale and it eventually provides the driving force for the translocation of protons. The elementary photoisomerization event proceeds on multiple coupled PESs; following the absorption of a photon, ground state population is transferred to the first excited state and the ensuing intramolecular dynamics finally lead to the transfer of excited state population back to the ground electronic state. This population transfer is expected to be most efficient in regions of the potential surface where the ground and excited states are nearly or exactly isoenergetic, for example at a CI.

In our previous studies [8,16], a simple three-state model was used to describe the photoisomerization process. The three PESs differed only in their dependence on one torsional coordinate: the angle  $\phi$  about the C<sub>13</sub>=C<sub>14</sub> double bond. Experimental evidence, which supports a three-state model, is available [17,18]. However, recent experimental [19–21] and theoretical [22–24] studies suggest that the initial motion out of the Franck–Condon region does not involve a torsional coordinate. Whereas our previous studies treated the crossing between the ground and excited state as an avoided crossing, these theoretical studies (of 11-*cis* retinal protonated analog) indicate that the decay back to the ground electronic state proceeds via a true crossing, i.e. a CI [23–25]. This could have a profound effect on the photodynamics since internal conversion is known to be extremely

efficient when CIs are encountered [26]. The description of CIs requires that the PES of the coupled electronic states differ in at least two coordinates, for example the  $C_{13}=C_{14}$  torsion (see Fig. 1) and bond stretching [22–24]. The theoretical investigation of the minimum energy path of the 11-*cis* analog [24] revealed that the initial motion on the first excited state involves skeletal (i.e. stretching) relaxation which is followed by a torsional motion. The present work differs from this study in two ways. First, while an 11-*cis* analog was previously used as a model for rhodopsin, we use an all-*trans* analog because we are interested in bR. Second, the analog used in the present study includes two additional methyl groups: one on the retinal backbone and one as a replacement of the Lys216 link of the chromophore (see Fig. 1). To our knowledge this is the largest RPSB analog model ever studied. However, we note that our model does not include the protein environment.

## 2. Methods

### 2.1. Quantum chemistry of the retinal Schiff base

A suitable description of electronic excited states in molecules, including retinal analogs and their protonated Schiff bases, requires an ab initio description accounting at least for static electron correlation. The complete active space (CAS) methods developed by Roos and coworkers [27] have been shown to provide an accurate account of these effects, and are often quantitatively accurate when supplemented by low-order perturbation corrections [28]. Since these methods are computationally very demanding, it is not yet feasible to carry out calculations on the retinal chromophore itself. However, calculations are possible for analogs slightly smaller than retinal. In particular, analogs which omit the beta-ionone ring have been widely used because this ring is likely to have only a small effect on the electronic behavior of the conjugated backbone [29]. Accordingly, we have chosen for the present study the model Schiff base all-*trans*-3,7-dimethylnona-2,4,6,8-tetraenmethyliminium cation shown in Fig. 1. This model includes ten conjugated  $\pi$  electrons as well as two pertinent methyl group on retinal's backbone, and an additional methyl groups that replaces the Lys216 link of the chromophore, but it neglects the beta-ionone ring.

All calculations were carried out with the program MOLPRO98 [30] using CASSCF in a  $\pi$  active space of ten electrons in ten orbitals and the 6-31G\* basis set [31,32]. A state-averaging procedure, equally weighting the two lowest states ( $S_0$  and  $S_1$ ), was used to determine the optimal CASSCF orbitals. This state-averaged (SA) CASSCF(10,10) wave-function includes a large portion of static correlation energy and it allows a satisfactory description of the first excited state. The chosen active space is large enough to include the most important configurations. This has been verified by rotating the orbitals bordering the active space and monitoring the ground and excited state energies, properties that were found to be unaffected. All calculations were done in vacuo and optimizations were carried out in the full space of geometrical coordinates. Using 2 Gbytes of RAM, a typical evaluation of energies and other properties (e.g. energy gradient, nonadiabatic coupling) for a single geometry required between 8 and 12 CPU hours on an SGI Origin2000 processor.

### 2.2. Minima and conical intersection

The SA-CASSCF(10,10) molecular geometry has been optimized on the ground and excited states. Convergence was reached when the norm of the gradient vector was less than  $10^{-6}$  a.u. For the ground state minimum, the search was started from the equilibrium geometry determined by a DFT/B3LYP calculation in the 6-31G\* basis set. Our search for the excited state minimum started from the ground state equilibrium geometry, with a  $90^\circ$  torsion induced around the  $C_{13}=C_{14}$  bond. The calculations therefore target the local minimum which is relevant to the all-*trans*  $\rightarrow$  13-*cis* isomerization process in bR. We have not searched for local minima corresponding to torsion about other double bonds, e.g. the  $C_{11}=C_{12}$  bond. However preliminary calculations suggest that, in the vicinity of the Franck–Condon region, the force constant for rotation around the  $C_{13}=C_{14}$  is lower than the force constants for rotations around the other (nominally) double bonds, e.g.  $C_{11}=C_{12}$  and  $C_9=C_{10}$ .

A search for the geometry of the CI was started from two different initial geometries, the  $S_0$  and  $S_1$  minima mentioned above, and converged to the same structure. The procedure involved at each point calculations of the gradient on the first excited

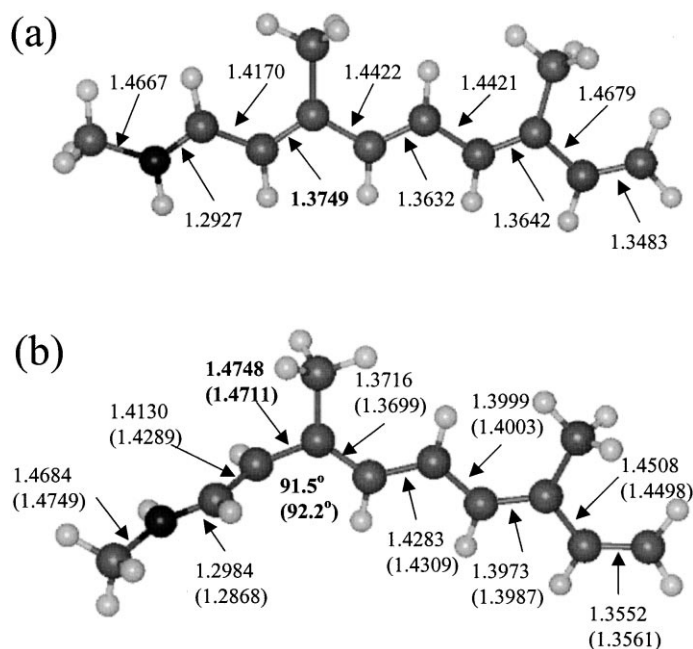


Fig. 2. Structures of the retinal analog at the minima of the ground ( $S_0$ ) and first excited ( $S_1$ ) state: (a) the compound at the  $S_0$  all-*trans* minimum is planar with reduced single/double bond alternation near the Schiff base; (b) the compound at the  $S_1$  minimum shows a  $91.5^\circ$  torsion around the  $C_{13}=C_{14}$  bond and a significant increase in this bond length. The structure at the  $S_1$  minimum nearly coincides with the structure at the lowest point of the conical intersection between  $S_1$  and  $S_0$ . Bond distances and angles are indicated in Å and degrees, and their values at the conical intersection are indicated in brackets.

state, the difference gradient between the  $S_0$  and  $S_1$  states (the  $\vec{h}$ -vector), and the nonadiabatic coupling vector (the  $\vec{g}$ -vector) between the two states [33,34]. The calculation of the  $\vec{g}$ -vector, as implemented in MOLPRO, neglects the geometry dependence of the molecular orbitals. In judging the corresponding errors one should recall that in the adiabatic representation there are two contributions to the derivative of the electronic wave-function with respect to the nuclear coordinates, one from the variation of the configuration interaction coefficients and a second from the variation of the molecular orbitals; since the molecular orbitals are determined with state averaging, their dependence on the nuclear coordinates is expected to be small and can be neglected.

Once the CI had been located, the ground and excited states PESs were mapped along the two coordinates that lift the degeneracy of the two states: the  $\vec{g}$ - and  $\vec{h}$ -vectors. The  $\vec{g}$ -vector was found to vary strongly in the vicinity of the CI, but it is always dominated by a component corresponding to torsion

around the  $C_{13}=C_{14}$  bond. We therefore chose this torsion along with the  $\vec{h}$ -vector as the two coordinates along which we sampled the ground and excited state PESs. We chose seven points along each direction, i.e. a total of 49 points with steps of  $10^\circ$  and 0.0716 Å.

### 3. Results

As described above we have used the program MOLPRO to identify the equilibrium geometries on the ground and excited electronic state, as well as the geometry corresponding to the lowest energy CI, for the retinal analog shown in Fig. 1. We have also explored the PESs in the vicinity of the CI. The results are described below.

#### 3.1. Potential energy surfaces

The equilibrium geometries of the ground and excited state of the RPSB analog investigated (see above) are depicted in panels (a) and (b) of Fig. 2.

Table 1  
Energies and energy differences of ground and excited states for the three structures discussed in the text

	$S_0$ minimum	$S_1$ minimum	CI
Hartree			
$S_0$	-519.19720829	-519.11743101	-519.11109212
$S_1$	-519.06832703	-519.11195824	-519.11099889
kcal/mol			
$S_0$	0.0	50.06	54.04
$S_1$	80.87	53.49	54.10
$S_1 - S_0$	80.87	3.43	0.06

The carbon backbone is completely planar in the ground state minimum (panel a) implying that any steric repulsion between the two methyl groups on the backbone is negligible. This should be contrasted with retinal in bR, where X-ray structures reveal significant deviations from planarity [6,7]. Our results suggest that nonplanar distortions of the retinal molecule in bR, and any resulting enhancements of bond selectivity in photoisomerization, must be ascribed to the influence of the protein environment. It is notable that bond alternation in the ground electronic state (panel a) is diminished near the Schiff base. The

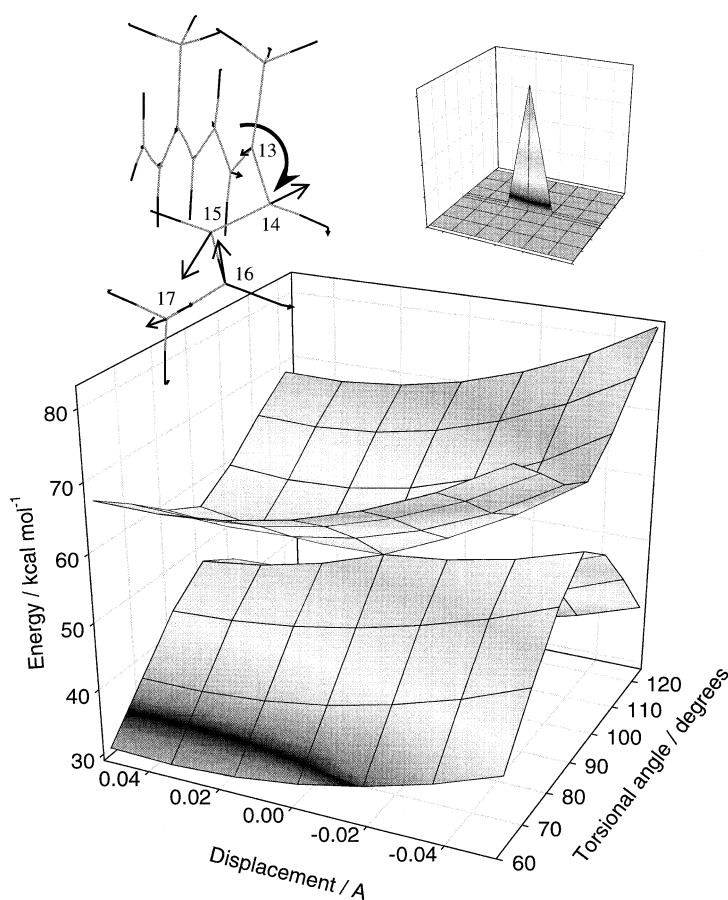


Fig. 3. Energies of the ground and first excited state of the retinal analog as a function of displacement along the  $\vec{h}$ -vector (in Å) and the  $C_{13}=C_{14}$  torsional angle (in degrees). All other coordinates are constrained to their values at the conical intersection and the zero of energy has been set to the ground state equilibrium value. The graphical rendering of the retinal analog depicts the  $\vec{h}$ -vector and the torsion, and the inset presents the magnitude of the nonadiabatic coupling as a function of the  $\vec{h}$ -vector and the  $C_{13}=C_{14}$  torsional angle.

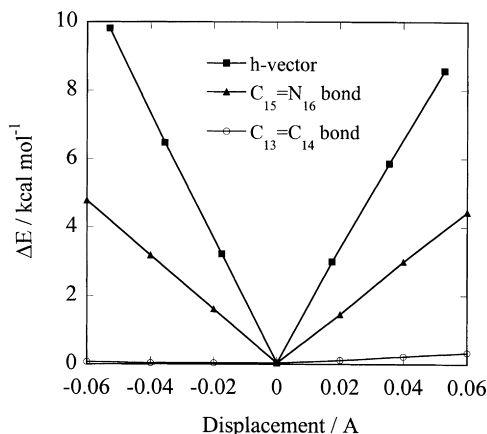


Fig. 4. Energy difference between the  $S_1$  and  $S_0$  states along the  $\vec{h}$ -vector, and as a function of the length of the  $C_{15}=N_{16}$  bond as well as of the  $C_{13}=C_{14}$  bond. (Other coordinates are constrained to their values at the conical intersection.)

length of the nominal single bond  $C_{14}=C_{15}$  measures 1.417 Å while the nominal double bond  $C_{13}=C_{14}$  measures 1.375 Å. The remaining bonds reflect a more typical bond alternation pattern. At the excited state equilibrium geometry the  $C_{13}=C_{14}$  double bond extends to 1.475 Å and it is rotated by 91.5°. Further changes between the ground and excited state involve mainly atoms  $C_{15}-C_{10}$ . For example, the nominal single bond  $C_{12}-C_{13}$  assumes a length of 1.372 Å and the adjacent nominal double bond  $C_{11}=C_{12}$  a length of 1.428 Å. The geometries in Fig. 2 suggest

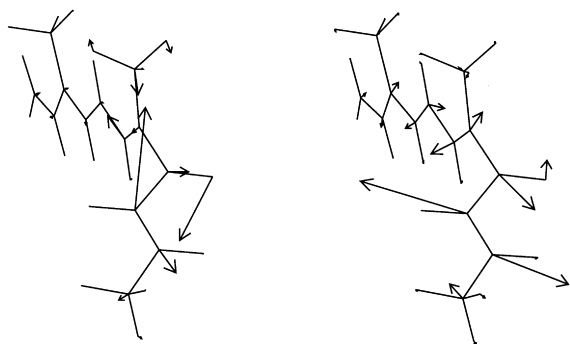


Fig. 5. The nonadiabatic coupling vector ( $\vec{g}$ -vector) for two geometries with very similar excited state energies and energy gaps between the ground and excited state. In both cases the magnitude of the nonadiabatic coupling is large ( $>300 \text{ bohr}^{-1}$ ), but apart from a common torsional component they are directed along different directions.

that the nearly perfect conjugation of the chromophore is broken in the excited state at the  $C_{13}=C_{14}$  bond, thereby, separating the molecule into two conjugated fragments.

A search for a CI was successful and located in very close proximity to the excited state equilibrium geometry. This is demonstrated in Fig. 2(b) where the respective torsional angles and bond lengths are compared (values in brackets correspond to the CI geometry). Not shown in this figure is a small, yet characteristic, difference between the CI and excited state equilibrium geometries; at the excited state equilibrium geometry the two methyl groups are aligned along the retinal backbone with two C–H bonds pointing towards each other, whereas at the CI the methyl at  $C_{13}$  is rotated by 2–4°.

Table 1 provides the energies in the ground and excited state for the three geometries described above. For our model compound the vertical excitation energy is 80.87 kcal/mol. At the  $S_1$  minimum the energy gap between the ground and excited state is only 3.43 kcal/mol, and at the CI this energy gap is further reduced to 0.06 kcal/mol; Table 1 shows that this change is predominantly due to a change in the ground state energy.

A Jahn–Teller (the most common type) exhibits two PESs touching each other in a cone and inverted cone fashion [34]. The two surfaces separate along the  $\vec{g}$  and  $\vec{h}$  vectors defined in Section 2. The  $\vec{g}$ – $\vec{h}$  plane represents the coordinates that are most effective in promoting nonadiabatic transitions. Fig. 3 demonstrates that the CI identified in this study is of a Jahn–Teller type. The PESs are shown along the  $\vec{h}$ -vector and along the torsion around the  $C_{13}=C_{14}$  bond. The surfaces separate very rapidly along the torsional coordinate and less rapidly along the  $\vec{h}$ -vector.

In the vicinity of the CI, we have also calculated the nonadiabatic coupling between the  $S_0$  and  $S_1$  states. The inset to Fig. 3 presents the results. One can recognize that the coupling is extremely localized near the CI, where it is singular (numerically, this coupling is computed to be larger than  $400 \text{ bohr}^{-1}$  at the CI).

The degrees of freedom involved in the  $\vec{h}$ -vector are depicted in the graphical rendering of the chromophore in Fig. 3. This vector involves a change in bond alternation localized around the last four backbone atoms ( $C_{14}$ ,  $C_{15}$ ,  $N_{16}$  and the terminal methyl group). The largest contribution is a stretch of the

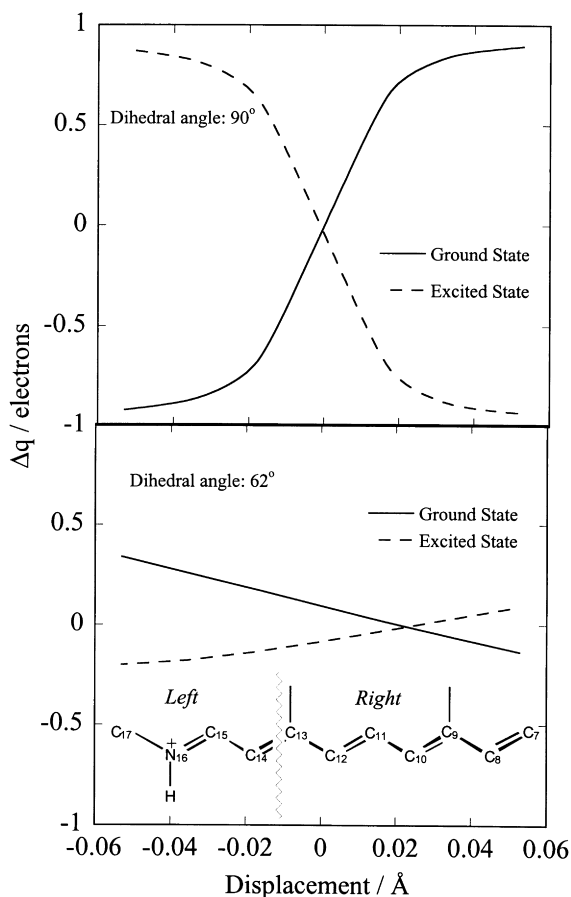


Fig. 6. Difference in charges of the left and right retinal analog fragments (computed using the Mulliken populations for the SA-CASSCF(10,10)/6-31G\* wavefunction) on the ground (full line) and first excited (dashed line) electronic state as a function of displacement along the  $\bar{h}$ -vector at two  $C_{13}=C_{14}$  torsional angles:  $90^\circ$  and  $62^\circ$  (upper and lower panels, respectively). (All other coordinates are constrained to their values at the conical intersection.) The inset illustrates the retinal analog and defines the right and left fragments: all atoms left of (and including)  $C_{14}$  belong to the left fragment whereas all atoms to the right of (and including)  $C_{13}$  belong to the right fragment.

$C_{15}=N_{16}$  bond, the two next largest contributions are from the contractions of the  $C_{14}=C_{15}$  and  $N_{16}$ -methyl bonds. A cut of the energy surfaces along the  $\bar{h}$ -vector is presented in Fig. 4. This figure also shows cuts along the  $C_{15}=N_{16}$  and  $C_{13}=C_{14}$  bond stretches. The behavior shown is surprising. Given the strong dependence of the PESs on the torsion around the  $C_{13}=C_{14}$  bond one would have expected the  $C_{13}=C_{14}$  bond

stretch to have a stronger effect than the  $C_{15}=N_{16}$  bond stretch. However, it is the latter bond stretch that induces a fast separation of the two PESs.

We also investigated the variation of  $\bar{g}$ -vector in the vicinity of the CI. As shown in Fig. 5 that conform the  $\bar{g}$ -vector at the CI and at a nearby point with similar energy and large nonadiabatic coupling, the  $\bar{g}$ -vector exhibits a strong change. In fact, apart from the common torsional component, the two vectors in Fig. 5 bear little resemblance. This behavior presumably reflects the strong curvature of the CI seam, but may also be partially due to numerical errors associated with the singular behavior of the nonadiabatic coupling at the CI.

The protonated Schiff base compound investigated (see Fig. 1) carries a net positive charge. In a well-conjugated system, one expects this charge to be distributed evenly over the compound. However, at the CI the conjugation is broken at the  $C_{13}=C_{14}$  bond due to a near  $90^\circ$  twist. We have investigated the distribution of the positive charge in the retinal analog by determining the difference  $\Delta q$  of the total Mulliken charges to the left and right of the center of the  $C_{13}=C_{14}$  bond. Fig. 6 shows  $\Delta q$  in the ground and excited state as a function of displacement along the  $\bar{h}$ -vector for the two torsional angles ( $90^\circ$  and  $62^\circ$ ). At the CI, the positive charge is completely delocalized in both ground and excited states. Small displacements along the  $\bar{h}$ -vector cause the hole to localize on one side of the  $90^\circ$  twisted  $C_{13}=C_{14}$  bond. When the torsion angle is more nearly planar ( $62^\circ$  shown), the delocalization of the hole becomes less sensitive to the displacement of the  $\bar{h}$ -vector. This suggests that a diabatic representation corresponding to this CI in the retinal molecule should focus on the two diabatic states corresponding to localization of the positive hole to the right or left of the  $C_{13}=C_{14}$  bond.

#### 4. Discussion

The results of our investigation suggest the following scenario for the photoreaction of the protonated Schiff base of retinal: following vertical excitation of the ground state equilibrium to the excited state the system moves out of the Franck–Condon region to the minimum of the excited state potential. This minimum is close to a CI that furnishes a gateway back

to the ground state potential energy surface. On this surface the system reaches either the isomerized state (13-*cis*) or the all-*trans* state. The CI which we have found is not exactly at a 90° twist around the C<sub>13</sub>=C<sub>14</sub> bond, implying a small preference for conversion back to the all-*trans* state. However, the deviation from a 90° torsion is small—the CI exhibits a 92° torsion. Hence the preference is expected to be quite minor and could easily be altered by the protein environment.

The motion from the Franck–Condon region to the excited state minimum involves torsion as well as bond stretch motion as indicated in Fig. 2. First, the initial motion changes the length of several backbone bonds, as has also been suggested in previous investigations [23,24] of an 11-*cis* retinal analog; this is followed by torsion towards a ca. 90° twist. Once the chromophore has arrived at the excited state minimum, the CI is reached rapidly through a slight rotation of the methyl group at C<sub>13</sub>.

At the CI, the nonadiabatic coupling is singular, leading to efficient internal conversion back to the ground state. The coordinates which are expected to be most effective in promoting this conversion are C<sub>15</sub>=N<sub>16</sub> stretch and C<sub>13</sub>=C<sub>14</sub> torsion, as suggested by the directions of the  $\vec{g}$ - and  $\vec{h}$ -vectors. The direction of the nonadiabatic coupling vector ( $\vec{h}$ ) is surprising in that it involves a dominant C<sub>15</sub>=N<sub>16</sub> stretch and only a small C<sub>13</sub>=C<sub>14</sub> stretch. Since overall both single and double bonds are displaced from their ground state equilibrium position at the CI, and neither one of them is involved in the direction of the nonadiabatic coupling vectors, one expects the ground state product (13-*cis*) and educt (all-*trans*) to be formed in a vibrationally excited state. (In this respect one should note that upon excitation the largest change in internuclear distance occurs at the C<sub>13</sub>=C<sub>14</sub> bond which stretches from 1.375 to 1.475 Å.) The surface crossing process requires an adequate quantum mechanical description of the nuclear motion, e.g. as suggested in [8,35], and will be the subject of future investigations.

A long standing question in the field of polyene photochemistry has been the selection of the bond undergoing isomerization. The present investigation has not addressed this point directly, focusing instead solely on the CI which is most relevant to the all-*trans* → 13-*cis* photoisomerization in bR. It is quite likely that there are other CIs corresponding to

isomerization about different C=C bonds, e.g. about the C<sub>11</sub>=C<sub>12</sub> bond. An understanding of the bond selectivity and, in particular, of the difference between photoproducts in solution and in bR [36–38] will require investigation of alternative CIs. In the present study, we did not find a barrier separating the Franck–Condon region from the excited state minimum, but cannot say with certainty that one does not exist. In particular, our procedure could easily miss a barrier of 600 cm<sup>-1</sup> as suggested by time-resolved studies of retinal photoisomerization in solution [39]. It is of great interest to understand how the protein environment can affect such a barrier and, hence, bond selectivity.

## Acknowledgements

This work was supported by the National Institutes of Health (NIH PHS 5 P41 RR05969), the National Science Foundation (BIR-9318159, BIR94-23827EQ), the MAC 93S028 computer-time grant and the Roy J. Carver Charitable Trust. T.J.M. is grateful to the NSF, Research Corporation, Beckman Foundation, and Sloan Foundation for their support through a Career Award, Research Innovation Award, Beckman Young Investigator Award, and a Sloan Fellowship, respectively.

## References

- [1] R.R. Birge, Photophysics and molecular electronic applications of the rhodopsins, *Annu. Rev. Phys. Chem.* 41 (1990) 683–733.
- [2] R.A. Mathies, S.W. Lin, J.B. Ames, W.T. Pollard, From femtoseconds to biology: mechanism of bacteriorhodopsin's light-driven proton pump, *Annu. Rev. Biochem. Bioeng.* 20 (1991) 491–518.
- [3] T. Ebrey, Light energy transduction in bacteriorhodopsin, in: M. Jacobson (Ed.), *Thermodynamics of Membranes, Receptors and Channels*, CRC, New York, 1993, p. 353–387.
- [4] J. Lanyi, Bacteriorhodopsin as a model for proton pumps, *Nature* 375 (1995) 461–463.
- [5] K. Schulten, W. Humphrey, I. Logunov, M. Sheves, Dong Xu, Molecular dynamics studies of bacteriorhodopsin's photocycles, *Isr. J. Chem.* 35 (1995) 447–464.
- [6] H. Belrhali, P. Nollert, A. Royant, C. Menzel, J.P. Rosenbusch, E.M. Landau, E. Pebay-Peyroula, Protein, lipid and water organization in bacteriorhodopsin crystals: a molecular view of the purple membrane at 1.9 Å resolution, *Structure* 7 (1999) 909–917.

- [7] H. Lücke, B. Schobert, H.T. Richter, J.P. Cartailier, J.K. Lanyi, Structure of bacteriorhodopsin at 1.55 Å resolution, *J. Mol. Biol.* 291 (1999) 899–911.
- [8] M. Ben-Nun, F. Molnar, Hui Lu, J.C. Phillips, T.J. Martínez, K. Schulten, Quantum dynamics of retinal's femtosecond photoisomerization in bacteriorhodopsin, *Faraday Discussions*, No. 110, December, Faraday Publications, 1998 (pp. 447–462).
- [9] W. Humphrey, I. Logunov, K. Schulten, M. Sheves, Molecular dynamics study of bacteriorhodopsin and artificial pigments, *Biochemistry* 33 (1994) 3668–3678.
- [10] W. Humphrey, Dong Xu, M. Sheves, K. Schulten, Molecular dynamics study of the early intermediates in the bacteriorhodopsin photocycle, *J. Phys. Chem.* 99 (1995) 14 549–14 560.
- [11] I. Logunov, W. Humphrey, K. Schulten, M. Sheves, Molecular dynamics study of the 13-*cis* form (bR<sub>548</sub>) of bacteriorhodopsin and its photocycle, *Biophys. J.* 68 (1995) 1270–1282.
- [12] Dong Xu, M. Sheves, K. Schulten, Molecular dynamics study of the M412 intermediate of bacteriorhodopsin, *Biophys. J.* 69 (6) (1995) 2745–2760.
- [13] Dong Xu, C. Martin, K. Schulten, Molecular dynamics study of early picosecond events in the bacteriorhodopsin photocycle: Dielectric response, vibrational cooling and the J, K intermediates, *Biophys. J.* 70 (1) (1996) 453–460.
- [14] W. Humphrey, E. Bamberg, K. Schulten, Photoproducts of bacteriorhodopsin mutants: a molecular dynamics study, *Biophys. J.* 72 (1997) 1347–1356.
- [15] E. Tajkhorshid, J. Baudry, K. Schulten, S. Suhai, Molecular dynamics study of the nature and origin of retinal's twisted structure in bacteriorhodopsin, *Biophys. J.* 78 (2000) 683–693.
- [16] W. Humphrey, H. Lu, I. Logunov, H.J. Werner, K. Schulten, Three electronic state model of the primary photo-transformation of bacteriorhodopsin, *Biophys. J.* 75 (1998) 1689–1699.
- [17] K.C. Hasson, Feng Gai, P.A. Anfinrud, The photoisomerization of retinal in bacteriorhodopsin: experimental evidence for a three-state model, *Proc. Natl. Acad. Sci., USA* 93 (1996) 15 124–15 129.
- [18] Feng Gai, K.C. Hasson, J.C. McDonald, P.A. Anfinrud, Chemical dynamics in proteins: the photoisomerization of retinal in bacteriorhodopsin, *Science* 279 (1998) 1886–1891.
- [19] I. Rouso, E. Khachatryan, Y. Gat, I. Brodski, M. Ottolenghi, M. Sheves, A. Lewis, Microsecond atomic force sensing of protein conformational dynamics: implications for the primary light-induced events in bacteriorhodopsin, *Proc. Natl. Acad. Sci., USA* 94 (1997) 7397–7941.
- [20] T. Ye, N. Friedman, Y. Gat, G.H. Atkinson, M. Sheves, M. Ottolenghi, S. Ruhman, On the nature of the primary light-induced events in bacteriorhodopsin: ultrafast spectroscopy of native and C<sub>13</sub>=C<sub>14</sub> locked pigments, *J. Phys. Chem.* 103B (1999) 5122–5130.
- [21] L. Song, M.A. El-Sayed, Primary step in bacteriorhodopsin photosynthesis: bond stretch rather than angle twist of its retinal excited-state structure, *J. Am. Chem. Soc.* 120 (34) (1998) 8889–8890.
- [22] T. Vreven, F. Bernardi, M. Garavelli, M. Olivucci, M.A. Robb, H.B. Schlegel, Ab initio photoisomerization dynamics of a simple retinal chromophore model, *J. Am. Chem. Soc.* 119 (1997) 12 687–12 688.
- [23] M. Garavelli, P. Celani, F. Bernardi, M.A. Robb, M. Olivucci, The C<sub>6</sub>H<sub>5</sub>NH<sub>2</sub><sup>+</sup> protonated Schiff base: an ab initio minimal model for retinal photoisomerization, *J. Am. Chem. Soc.* 119 (1997) 6891–6897.
- [24] M. Garavelli, T. Vreven, P. Celani, F. Bernardi, M.A. Robb, M. Olivucci, Photoisomerization path for a retinal chromophore model: the nonatetraeniminium cation, *J. Am. Chem. Soc.* 120 (1998) 1285–1288.
- [25] V. Bonacic-Koutecky, K. Schoffel, J. Michl, Critically heterosymmetric biradicaloid geometries of the protonated Schiff bases, *Theor. Chim. Acta* 72 (1987) 459–474.
- [26] M. Klessinger, J. Michl, *Excited States and Photochemistry of Organic Molecules*, VCH, New York, 1995.
- [27] B.O. Roos, The complete active space self-consistent field method and its applications in electronic structure calculations, in: K.P. Lawley (Ed.), *Advances in Chemical Physics; Ab Initio Methods in Quantum Chemistry-II*, Wiley, New York, 1987, pp. 399–445.
- [28] B.O. Roos, Theoretical studies of electronically excited states of molecular systems using multiconfigurational perturbation theory, *Acc. Chem. Res.* 32 (1999) 137–144.
- [29] R.A. Poirier, A. Yadav, P.R. Surjan, Preliminary ab initio investigation of retinal analogs, *J. Mol. Struct. (Theochem)* 167 (1988) 321–329.
- [30] H.-J. Werner, P.J. Knowles, with contributions from R.D. Amos, A. Berning, D.L. Cooper, M.J.O. Deegan, A.J. Dobbyn, F. Eckert, C. Hampel, T. Leininger, R. Lindh, A.W. Lloyd, W. Meyer, M.E. Mura, A. Nicklass, P. Palmieri, K. Peterson, R. Pitzer, P. Pulay, G. Rauhut, M. Schütz, H. Stool, A.J. Stone, T. Thorsteinsson, *MOLPRO—ab initio programs*.
- [31] H.-J. Werner, P.J. Knowles, Second order multiconfiguration SCF procedure with optimum convergence, *J. Chem. Phys.* 82 (1985) 5053–5063.
- [32] P.J. Knowles, H.-J. Werner, An efficient second-order MC SCF method for long configuration expansions, *Chem. Phys. Lett.* 115 (1985) 259–267.
- [33] D.R. Yarkony, Diabolic conical intersections, *Rev. Mod. Phys.* 68 (1997) 985–1013.
- [34] D.R. Yarkony, Conical intersections: diabolic and often misunderstood, *Acc. Chem. Res.* 31 (1998) 511–518.
- [35] M. Ben-Nun, T.J. Martínez, Validation of the multiple spawning method for nonadiabatic dynamics in a multidimensional model problem, *J. Chem. Phys.* 108 (1998) 7244–7257.
- [36] K.A. Freedman, R.S. Becker, Comparative investigation of the photoisomerization of the protonated and unprotonated *n*-butylamine Schiff bases of 9-*cis*–11-*cis*, and all-*trans*-retinals, *J. Am. Chem. Soc.* 108 (1986) 1245–1251.
- [37] Y. Koyama, K. Kubo, M. Komori, H. Yasuda, Y. Mukai,

Effect of protonation on the isomerization properties of *n*-butylamine Schiff base of isomeric retinal as revealed by direct HPLC analyses: selection of isomerization pathways by retinal proteins, *Photochem. Photobiol.* 54 (1991) 433–443.

[38] M. Ben-Nun, T.J. Martínez, Electronic energy funnels in *cis*–

*trans* photoisomerization of retinal protonated Schiff base, *J. Phys. Chem.* 102A (1998) 9607–9617.

[39] S.L. Logunov, L. Song, M.A. El-Sayed, Excited-state dynamics of a protonated retinal Schiff base in solution, *J. Phys. Chem.* 100 (1996) 6–18 591.